

Upconversion fluorescence modulation of CaTiO₃: Yb³⁺/Er³⁺ nanocubes via Zn²⁺ introduction*

MU Jiajia, LIU Jinyu, and GAO Lili**

School of Science, Beihua University, Jilin 132013, China

(Received 4 August 2021; Revised 20 September 2021)

©Tianjin University of Technology 2022

To investigate the effect of Zn²⁺ ions on the luminescence properties of rare earth (RE) doped calcium titanate materials, CaTiO₃: Yb³⁺/Er³⁺/Zn²⁺ nanocubes with uniform size were prepared by solvothermal method in this paper. They were respectively characterized by X-ray diffractometer (XRD), scanning electron microscope (SEM), photoluminescence (PL) spectroscopy and their fluorescence lifetimes. The results show that the average size of the nanocubes is about 550 nm×650 nm×850 nm with good upconversion luminescence (UCL) properties. Under 980 nm laser excitation, the effects of the ratio between activator Er³⁺ and sensitizer Yb³⁺ and Zn²⁺ doping on the upconversion fluorescence properties were investigated, and the optimal ion ratio was obtained. The results of steady-state spectra show that the strongest fluorescence intensity of CaTiO₃: Yb³⁺/Er³⁺ was obtained with the addition of 10 mol% Zn²⁺ at a Yb³⁺/Er³⁺ molar doping ratio of 3:0.3, which was attributed to the crystal field asymmetry generated by the introduction of Zn²⁺ ions. The energy transfer and upconversion mechanism between Yb³⁺ and Er³⁺ ions in CaTiO₃ nanocubes were investigated by analyzing the upconversion fluorescence kinetics.

Document code: A **Article ID:** 1673-1905(2022)03-0129-6

DOI <https://doi.org/10.1007/s11801-022-1125-7>

The particular spectroscopic properties of rare earth (RE) ions in different host lattices are widely applied in solid state lighting^[1], sensors^[2], light emitting diode (LED)^[3] and biomedical diagnosis agents^[4]. Recently, perovskite ATiO₃ (A=Ca, Ba, Sr) has attracted significant attention due to excellent physical and chemical properties and promising applications in the photocatalysts^[5], optoelectronic devices^[6], temperature sensors^[7], and biomedical field^[8]. Doping RE ions into ATiO₃ can exhibit numerous advantages in optical properties, including low power consumption, high luminescence efficiency and environmental friendliness^[9,10]. It is evident that efficient upconversion luminescence (UCL) can be obtained by introducing RE ions Yb³⁺ and Er³⁺ as sensitizers and activators with ATiO₃ as matrix materials^[11,12]. Among them, calcium titanate with phonon energy less than 700 cm⁻¹ is considered to be a promising fluorescent substrate and has been extensively investigated in the fields of optics, piezoelectricity, magnetism, gas sensitivity and catalysis^[13-17].

Recently, significant efforts have been made to enhance the UCL of CaTiO₃ through co-doping. The UCL intensity of RE ions is not only related to the matrix phonon energy, but also to the crystal field environment of RE ions. The doping of inactive ions to reduce the crystal field symmetry of RE ions can increase the

chance of RE ion radiative transition and improve the UCL intensity. In recent years, the research has gradually increased on enhancing the upconversion emission intensity by doping transition metal Zn²⁺ ions. MAHATA et al^[18] have synthesized Zn²⁺ doping BaTiO₃: Er³⁺/Yb³⁺ nanophosphor with the prominent luminescence properties by a wet-chemical co-precipitation route. Zn-doped CaTiO₃: Eu³⁺ red phosphors have been prepared by WU for enhanced photoluminescence in white LEDs^[6]. WANG et al^[19] have obtained a Ca_{1-x}Zn_xTiO₃: Eu³⁺ red phosphor with higher luminescence intensity that was closer to standard red light. The reason for these enhancements is that the transition metal ions co-doped into the matrix may occupy the substitution site, gap site or grain boundary, which may affect the emission intensity of phosphors. It has been shown that doping Zn²⁺ in the matrix can improve the photoluminescence performance^[5]. However, the luminescence performance of Zn²⁺-doped CaTiO₃: Yb³⁺/Er³⁺ nanocubes has not been fully investigated. Therefore, CaTiO₃: Yb³⁺/Er³⁺ nanophosphor doped with Zn²⁺ ions was designed to get high UCL through modulating the local crystal field around Er³⁺ ions and breaking the symmetry of the crystal field around the RE ions in the paper.

We used the solvothermal method to prepare Zn²⁺-doped CaTiO₃: Yb³⁺/Er³⁺ nanocubes. This method

* This work has been supported by the Jilin Science and Technology Development Program (No.20170520108JH), the Innovation Training Program for Undergraduates of Beihua University (No.202110201040), and the Transverse Project of Beihua University of Design and Preparation of New Functional Materials.

** E-mail: llgaobh@163.com

was combined with annealing techniques to prepare nanocubes that were uniform in size and easily doped with RE ions, as described in Refs.[20] and [21]. YANG et al^[20] used this method to prepare $\text{CaTiO}_3:\text{Pr}^{3+}$ nanocubes and demonstrated excellent photoluminescence. However, the preparation of upconversion nanocubes based on this method has rarely been reported. In this paper, we explained the formation mechanism of Zn^{2+} -doped $\text{CaTiO}_3:\text{Yb}^{3+}/\text{Er}^{3+}$ nanocubes and characterized their morphology and UCL properties. The effects of different contents of RE ions and Zn^{2+} ions were investigated in detail on the photoluminescence properties of $\text{CaTiO}_3:\text{Yb}^{3+}/\text{Er}^{3+}$. The results showed that when $\text{Yb}^{3+}/\text{Er}^{3+}=10:1$ and Zn^{2+} content was 10 mol%, the strong fluorescence emission was shown and the red-to-green ratio (R/G) was maximum. By changing the doping amounts of Yb^{3+} and Er^{3+} ions, the luminescence performance and R/G can be significantly changed. The mechanism of Zn^{2+} doping enhanced UCL was analyzed and determined in detail.

In typical synthesis, 4 mol/L $\text{Ca}(\text{NO}_3)_2 \cdot 4\text{H}_2\text{O}$, 0.2 mol/L $\text{Yb}(\text{NO}_3)_3 \cdot 6\text{H}_2\text{O}$, 0.2 mol/L $\text{Er}(\text{NO}_3)_3 \cdot 6\text{H}_2\text{O}$, 0.2 mol/L $\text{Zn}(\text{NO}_3)_2 \cdot 6\text{H}_2\text{O}$, 0.33 mL of tetrabutyl titanate and sodium hydroxide solution were dissolved in PEG-200 solvent, then the solution was stirred at room temperature for 1 h. Subsequently, the mixture solution was solvothermally treated at 180 °C for 15 h and sintered at 700 °C for 2 h.

The crystallinity and structures were analyzed by a Smart Lab X-ray diffractometer (XRD) with Cu K α radiation ($\lambda=1.54056 \text{ \AA}$) in a range of diffraction angle between 20° and 80° at a scanning rate of 6.0°/min. The morphology of the products was determined using a FEI/Nova Nano scanning electron microscope (SEM) 450. The UCL and pump power dependence measurements were obtained by a Hitachi F-7000 luminescence spectrometer with 980 nm excitation light source. The fluorescence decay lifetimes were recorded with a Triax 550 spectrometer (Jobin-Yvon). All the measurements were performed at room temperature.

Fig.1(a) shows the SEM image of the surface morphology of $\text{CaTiO}_3:\text{Yb}^{3+}/\text{Er}^{3+}/\text{Zn}^{2+}$ nanocubes synthesized by the solvothermal method and annealed at 700 °C. As seen in Fig.1(a), the nanocube scale is about 550 nm×650 nm×850 nm, and Fig.1(b) presents XRD patterns of the $\text{CaTiO}_3:15 \text{ mol\% Yb}^{3+}/1 \text{ mol\% Er}^{3+}$ (M1) and $\text{CaTiO}_3:3 \text{ mol\% Yb}^{3+}/0.3 \text{ mol\% Er}^{3+}/17 \text{ mol\% Zn}^{2+}$ (M2). The XRD spectra of both samples show that the structure matches with the CaTiO_3 standard card (JCPDS No.82-0228), indicating that the nanocube $\text{CaTiO}_3:\text{Yb}^{3+}/\text{Er}^{3+}/\text{Zn}^{2+}$ structure can be obtained by the process of this series. The growth mechanism of this system has been reported^[22]. In this paper, $\text{Ca}(\text{NO}_3)_2$, $\text{Yb}(\text{NO}_3)_3$, $\text{Er}(\text{NO}_3)_3$, and NaOH used are all aqueous solutions, and water is introduced into the system, which causes the nanocubes to aggregate directionally and form the final configuration of the cube. Then, after calcination out, the luminescence properties and crystal structure are significantly improved.

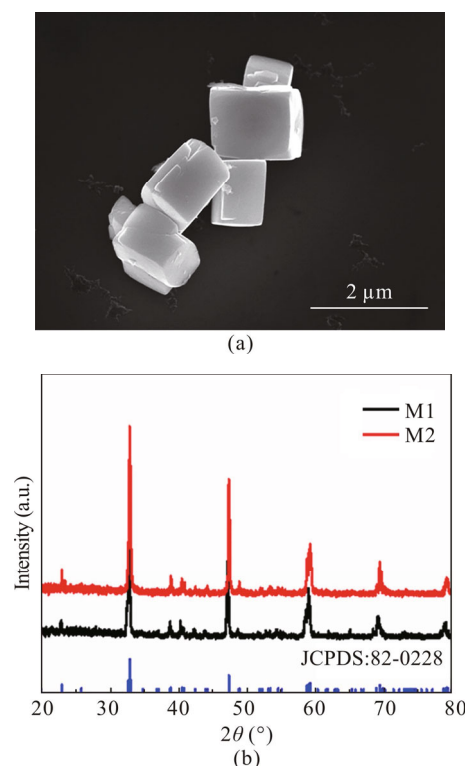


Fig.1 (a) SEM image of $\text{CaTiO}_3:\text{Yb}^{3+}/\text{Er}^{3+}/\text{Zn}^{2+}$ nanocubes; (b) XRD patterns of $\text{CaTiO}_3:\text{Yb}^{3+}/\text{Er}^{3+}/\text{Zn}^{2+}$ nanocubes

In this paper, the luminescence performance of upconversion luminescent materials is regulated through changing the ratio between internal activator Er^{3+} and sensitizer Yb^{3+} and doping Zn^{2+} ions. Fig.2(a) shows the upconversion fluorescence spectra of five $\text{CaTiO}_3:1 \text{ mol\% Er}^{3+}/x \text{ mol\% Yb}^{3+}$ ($x=3, 6, 10, 15, 20$) nanocubes structured sintered samples, the light source used was a 980 nm infrared laser, and the concentration of Er^{3+} ions was fixed and the concentration of Yb^{3+} ions was varied. The dazzling upconversion fluorescence is visible under continuous laser excitation at 980 nm. The emissions of $\text{CaTiO}_3:\text{Yb}^{3+}/\text{Er}^{3+}$ phosphors can be attributed to the f-f transitions from $^2\text{H}_{11/2}/^4\text{S}_{3/2}$ and $^4\text{F}_{9/2}$ states to $^4\text{I}_{15/2}$ ground state of Er^{3+} ions, where the green and red UCL peaks in the spectrum are located at 526 nm, 544 nm and 662 nm, respectively, corresponding to the Er^{3+} ion. The UCL emission of Er^{3+} intensely counts on the Yb^{3+} content, and the amount of doping in the activated luminescence center also affects its luminescence performance. The experimental results show that the intensity of $^2\text{H}_{11/2} \rightarrow ^4\text{I}_{15/2}$ (526 nm), $^4\text{S}_{3/2} \rightarrow ^4\text{I}_{15/2}$ (544 nm) and $^4\text{F}_{9/2} \rightarrow ^4\text{I}_{15/2}$ (662 nm) increases significantly with the increase of Yb^{3+} content under 980 nm excitation with fixed Er^{3+} content as shown in Fig.2(b). The maximum R/G ratio was observed when the content of Yb^{3+} was 15 mol%, as shown in Fig.2(c). The intensity of luminescence increases on account of the energy transfer from Yb^{3+} to Er^{3+} , but it decreased with the Yb^{3+} content exceeded 15 mol%, because of the variation in the local field of Er^{3+} ions, which hindered the non-radiative jump of Er^{3+} ($^2\text{H}_{11/2}/^4\text{S}_{3/2} \rightarrow ^4\text{F}_{9/2}$), resulting in the decrease

of the red luminescence intensity of Er^{3+} ($^4\text{F}_{9/2} \rightarrow ^4\text{I}_{15/2}$). In addition, we gradually increased the Er^{3+} content from 0.5 mol% to 2.5 mol% while keeping the Yb^{3+} content constant, the decrement in intensity corresponding to the effect of concentration quenching, as shown in Fig.3. The maximum R/G ratio was observed when the content of Er^{3+} was 1 mol%, and then decreased apparently. The possible reason was that the cross-relaxation mechanism of $\text{Yb}^{3+}-\text{Er}^{3+}$ ($^4\text{F}_{7/2} \rightarrow ^4\text{I}_{11/2}$ and $^2\text{F}_{5/2} \leftarrow ^2\text{F}_{7/2}$) appeared with Er^{3+} doping content increased from 0.5 mol% to 1 mol%. This led to additionally filling the $^4\text{F}_{9/2}$ state. Meanwhile, the space between adjacent Er^{3+} ions became smaller, which promoted energy transfer and resulted in quenching effect.

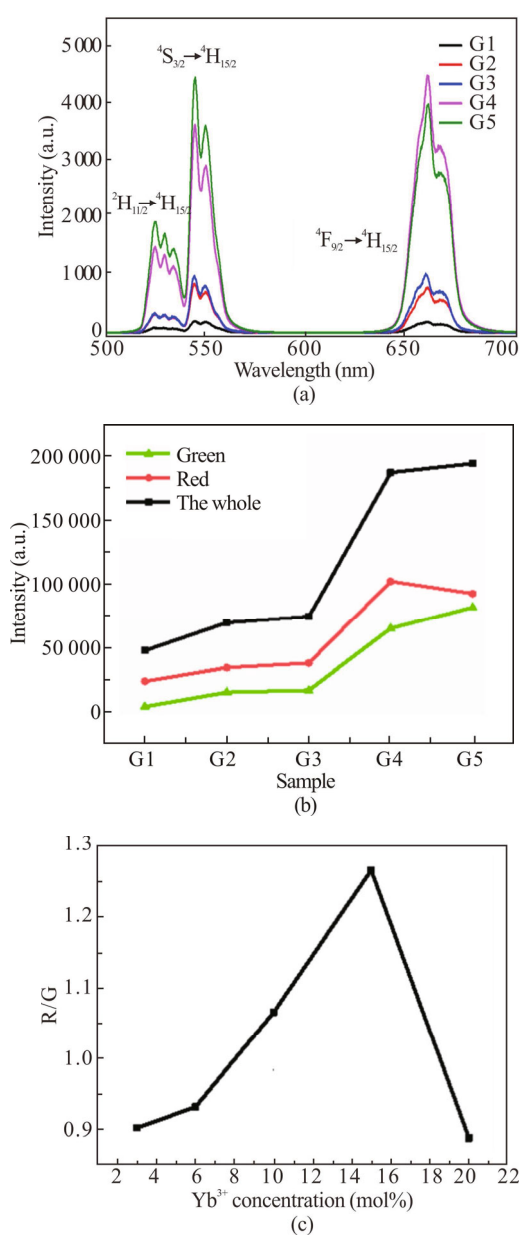


Fig.2 (a) Upconversion emission spectra for CaTiO_3 : 1 mol% Er^{3+}/x mol% Yb^{3+} ($x=3, 6, 10, 15, 20$) (G1: $x=3$; G2: $x=6$; G3: $x=10$; G4: $x=15$; G5: $x=20$); (b) Integrated intensities of red, green and overall upconversion emissions; (c) R/G versus Yb^{3+} content

Considering that the UCL intensity of RE ions is also related to the crystal field environment, the symmetry of the local crystal field around the RE ions can be released by doping the matrix with transition metal ions, which can increase the chance of RE ion radiative transition and improve the UCL intensity. Considering the large doping amount of Zn^{2+} ions, the appropriate concentrations of Er^{3+} and Yb^{3+} ions are 0.3 mol% and 3 mol%, respectively in order to avoid the impurity of calcium titanate phase caused by excessive doping concentration.

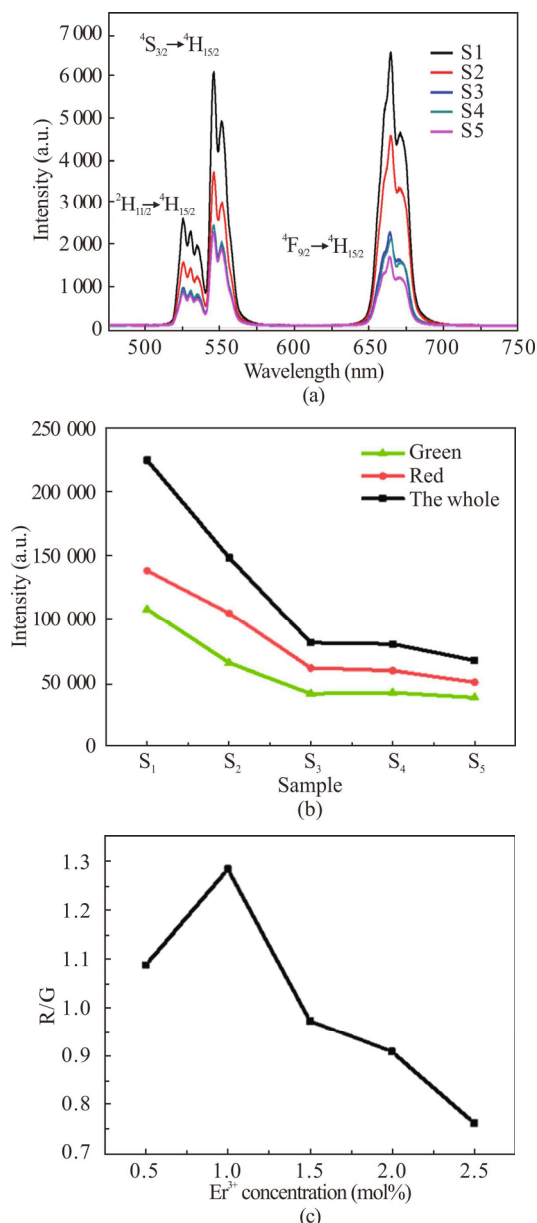


Fig.3 (a) Upconversion emission spectra for CaTiO_3 : 10 mol% Yb^{3+}/y mol% Er^{3+} ($y=0.5, 1, 1.5, 2, 2.5$) phosphors (S1: $y=0.5$; S2: $y=1$; S3: $y=1.5$; S4: $y=2$; S5: $y=2.5$); (b) Integrated intensities of red, green and overall upconversion emissions; (c) R/G versus Er^{3+} content

As shown in Fig.4, the upconversion emission spectra of $\text{CaTiO}_3: \text{Yb}^{3+}/\text{Er}^{3+}$ without Zn^{2+} doping and that with

Zn²⁺ doping were obtained using 980 nm laser excitation. The emission bands of Er³⁺ ions are clearly presented under 980 nm laser excitation: ²H_{11/2}→⁴I_{15/2} (526 nm), ⁴S_{3/2}→⁴I_{15/2} (544 nm) and ⁴F_{9/2}→⁴I_{15/2} (662 nm). Apparently, the spectral configurations of CaTiO₃: Yb³⁺, Er³⁺, Zn²⁺ kept unchanged but a significant change in intensity. The inset of Fig.4(b) shows the relative intensity integrated area and the overall fluorescence intensity integrated area of ⁴F_{9/2}→⁴I_{15/2} versus ²H_{11/2}/⁴S_{3/2}→⁴I_{15/2} in relation to the Zn²⁺ co-doping content, from which it can be seen that the emission intensity of green and red light gradually increases for the Zn²⁺-doped sample compared to the sample without Zn²⁺ doping. The UCL intensity is the strongest when the Zn²⁺ co-doping content is 10 mol%. When the symmetry crystal field around the RE ions is lower, the possibility of radiative transition is greater, and the Zn²⁺ doping breaks the symmetry of the local crystal field, so the UCL is greatly enhanced. As the doping concentration of Zn²⁺ continues to increase, the luminescence intensity declined as a result of the possible dilution effect. When increasing the Zn²⁺ content, the lattice deformation and much long distance between Yb³⁺ and Er³⁺ ions appear. Meanwhile, the R/G ratio also increased from 1.0 to the maximum value 1.7 with increasing the Zn²⁺ content from 0 to 15 mol%. However, when the Zn²⁺ content was further increased from 15 mol% to 17 mol%, the R/G ratio decreased. At 980 nm excitation, the doping of Zn²⁺ could induce an additional population of the ⁴F_{9/2} energy level through a radiation-free relaxation process at the ²H_{11/2} and ⁴S_{3/2} energy levels. However, when the Zn²⁺ concentration increases from 15 mol% to 17 mol%, the R/G ratio decreases as shown in Fig.4(c), which may be due to the dilution effect of the large amount of Zn²⁺ introduced into the perovskite lattice.

Since the size of Zn²⁺ ions is smaller than that of Ca²⁺ ions, Zn²⁺ ions can replace Ca²⁺ ions at low Zn²⁺ concentrations (≤20 mol%)^[12]. The results show that Zn²⁺ easily moves and localizes in the CaTiO₃ lattice, which leads to possible lattice defects. The maximum value reaches at a Zn²⁺ doping content of 10 mol% owing to the symmetric release of the local crystal field around RE ions. When the Zn²⁺ content is up to 15 mol%, the UCL intensity decreases due to the dilution effect of Zn²⁺, which leads to lattice distortion and excessive distances of Yb³⁺ and Er³⁺ ions. This suggests that doping with Zn²⁺ ions could provide a way to change the symmetry of the local crystal field, which would significantly affect the electron hopping possibility of the lanthanide ions and thus UCL intensity was improved.

To further understand the upconversion photon excitation mechanism, the upconversion log-log plots of intensity dependence of CaTiO₃: 3 mol% Yb³⁺/0.3 mol% Er³⁺/15 mol% Zn²⁺ with a 980 nm excitation are shown in Fig.5. For nonlinear effects, the UCL intensities $I(P)$ are related to the input power P^n , according to the expression $I(P) \propto P^n$, where n stands for the number of pump photons. Fig.5 shows the emission intensity and overall emission of ²H_{11/2}/⁴S_{3/2}→⁴I_{15/2} (green), ⁴F_{9/2}→⁴I_{15/2} (red)

at different excitation power densities. The slopes of CaTiO₃: 3 mol% Yb³⁺/0.3 mol% Er³⁺/15 mol% Zn²⁺ samples are 1.82, 1.73 and 2.00, respectively, which indicates that the red, green and overall upconversion fluorescences are all two-photon absorption processes.

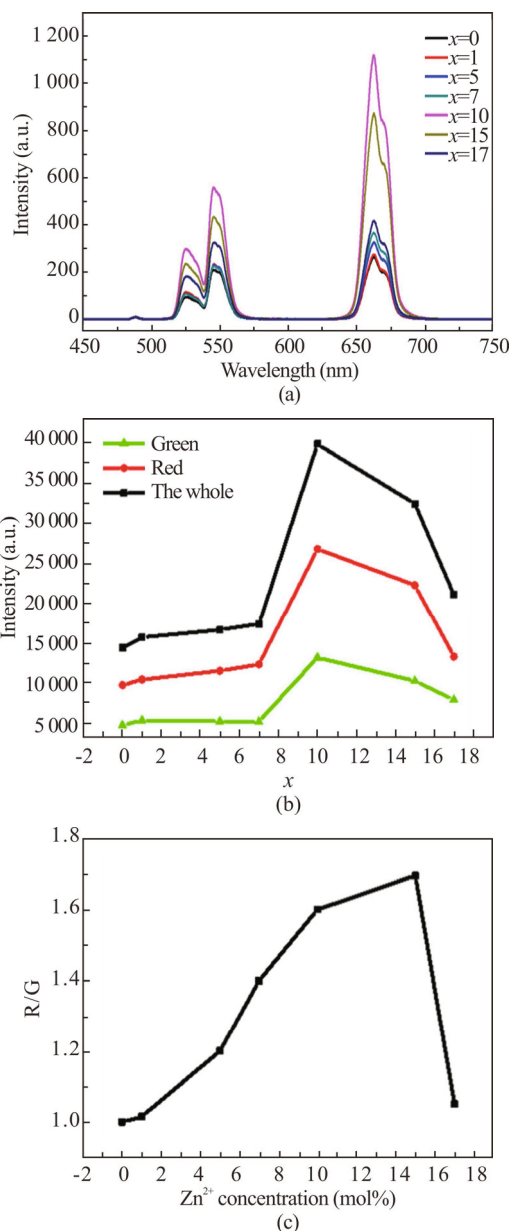


Fig.4 (a) Upconversion emission spectra for CaTiO₃: 3 mol% Yb³⁺/0.3 mol% Er³⁺/x mol% Zn²⁺ (x=0, 1, 5, 7, 10, 15, 17) phosphors; (b) Integrated intensities of red, green and overall upconversion emissions; (c) R/G versus Zn²⁺ content

The fluorescence decay lifetimes for the Er³⁺: ⁴S_{3/2} and ⁴F_{9/2} states with and without Zn²⁺ doping are shown in Fig.6. It shows the Er³⁺ (⁴S_{3/2}→⁴I_{15/2}) leap and (⁴F_{9/2}→⁴I_{15/2}) leap of different samples for the luminescence decay processes. The UCL lifetimes of ⁴S_{3/2} and ⁴F_{9/2} are 9.6 μs and 11.6 μs, respectively, and 20.9 μs and 21.9 μs, respectively. The UCL lifetime of Zn²⁺-doped CaTiO₃: Yb³⁺/Er³⁺

is prolonged by the entry of Zn^{2+} ions into the $CaTiO_3$ lattice, which can be seen that Zn^{2+} can break the symmetry of the crystal field around the RE ions, thus improving the UCL decay lifetime of Er^{3+} . In fact, the fluorescence lifetime is related to the sum of W_r (radiative leap probability) and W_n (non-radiative leap probability) according to the expression $\tau_d \propto 1/(W_r+W_n)$. It is observed that with increasing Zn^{2+} content from 0 to 10 mol%, the decay lifetimes increase well, indicating that the non-radiative leap probability decreases when Zn^{2+} ions are doped into the calcium titanate lattice. Therefore, it is clear that Zn^{2+} doping can influence W_n , which leads to longer decay lifetime.

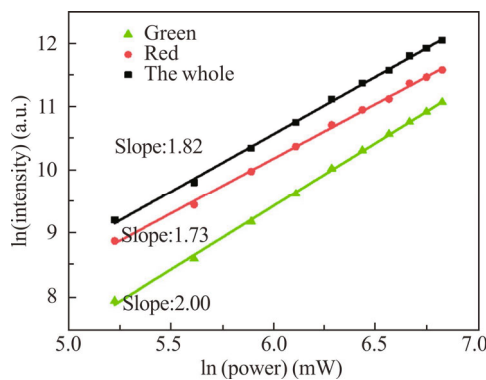


Fig.5 Pump power dependence of the red, green and the whole intensities of upconversion nanocubes

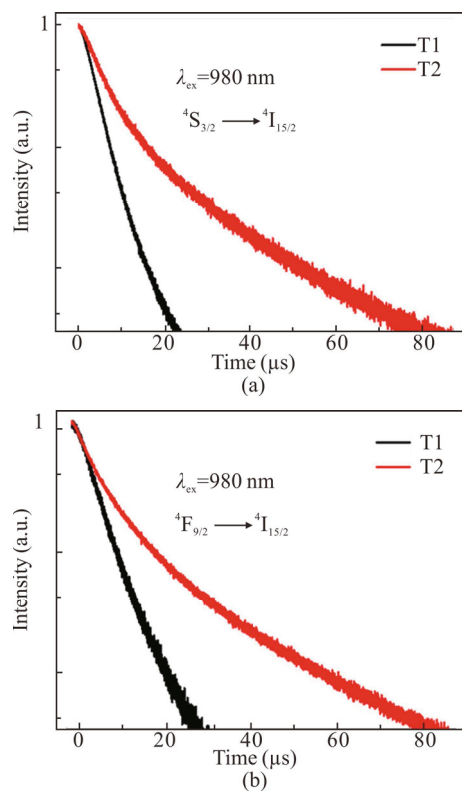


Fig.6 (a) Decay curves of green emission of the two samples; (b) Decay curves of red emission of the two samples (T1: $CaTiO_3$: 3 mol% Yb^{3+} /0.3 mol% Er^{3+} ; T2: $CaTiO_3$: 3 mol% Yb^{3+} /0.3 mol% Er^{3+} /15 mol% Zn^{2+})

RE doped $CaTiO_3$: $Yb^{3+}/Er^{3+}/Zn^{2+}$ phosphors were synthesized by a solvothermal method combined with annealing. In the calcium titanate matrix, the luminescence properties of the upconverted luminescent materials were adjusted by regulating the ratio between the internal activator Er^{3+} and the sensitizer Yb^{3+} on the one hand, and by adding transition group Zn^{2+} ions on the other hand. The R/G ratio was maximized when the ratio between the sensitizer Yb^{3+} and the activator Er^{3+} was 15:1. In the local crystal field where Zn^{2+} is introduced to regulate the activator, Zn^{2+} co-doping can release RE ions to affect the symmetry of the surrounding crystal field, thus improving the UCL efficiency and making the R/G ratio exhibit strong red light emission. Therefore, it is of great significance to prepare $CaTiO_3$: $Yb^{3+}/Er^{3+}/Zn^{2+}$ phosphors with excellent luminescence and chemical properties. Its upconversion enhancement characteristics are conducive to improve the luminous efficiency of LEDs. Due to the biocompatibility of the system, it can be used for the staining of animal cells, and then applied to the optical imaging of biological systems. It has potential application prospects in the fields of LEDs, biological cell luminescence probes and medical imaging.

Statements and Declarations

The authors declare that there are no conflicts of interest related to this article.

References

- [1] VERMA S, VERMA K, KUMAR D, et al. Recent advances in rare earth doped alkali-alkaline earth borates for solid state lighting applications[J]. *Physica B: condensed matter*, 2018, 535: 106-113.
- [2] TRIPATHI S, TIWARI R, SHRIVASTAVAA K, et al. A review reports on rare earth activated $AZrO_3$ (A = Ba, Ca, Sr) phosphors for display and sensing applications[J]. *Optik*, 2018, 157: 365-381.
- [3] GUPTA I, SINGH S, BHAGWAN S, et al. Rare earth (RE) doped phosphors and their emerging applications: a review[J]. *Ceramics international*, 2021, 47(14): 19282-19303.
- [4] LI Y, WANG R, ZHENG W, et al. Silica-coated Ga(III)-doped ZnO: Yb^{3+} , Tm^{3+} upconversion nanoparticles for high-resolution in vivo bioimaging using near-infrared to near-infrared upconversion emission[J]. *Inorganic chemistry*, 2019, 58(12): 8230-8236.
- [5] WANG R, NI S, LIU G, et al. Hollow $CaTiO_3$ cubes modified by La/Cr co-doping for efficient photocatalytic hydrogen production[J]. *Applied catalysis B: environmental*, 2018, 225: 139-147.
- [6] WU Y B, ZHAO F Y, PIAO X Q, et al. Zn-doped $CaTiO_3$: Eu^{3+} red phosphors for enhanced photoluminescence in white LEDs by solid-state reaction[J]. *Luminescence*, 2016, 31(1): 152-157.
- [7] JAIN N, SINGHR K, SINGHB P, et al. Enhanced temperature-sensing behavior of Ho^{3+} - Yb^{3+} -codoped $CaTiO_3$

- and its hybrid formation with Fe₃O₄ nanoparticles for hyperthermia[J]. ACS Omega, 2019, 4(4): 7482-7491.
- [8] LI X, ZHANG Q, AHMAD Z, et al. Near-infrared luminescent CaTiO₃: Nd³⁺ nanofibers with tunable and trackable drug release kinetics[J]. Journal of materials chemistry B, 2015, 37: 7449-7456.
- [9] TANG P, TOWNER D J, MEIER A L, et al. Low-voltage, polarization-insensitive, electro-optic modulator based on a polydomain barium titanate thin film[J]. Applied physics letters, 2004, 85(20): 4615-4617.
- [10] FASASIA Y, MAAZA M, ROHWERE G, et al. Effect of Zn-doping on the structural and optical properties of BaTiO₃ thin films grown by pulsed laser deposition[J]. Thin solid films, 2008, 516(18): 6226-6232.
- [11] MENG L, ZHANG K F, PAN K, et al. Controlled synthesis of CaTiO₃: Ln³⁺ nanocrystals for luminescence and photocatalytic hydrogen production[J]. RSC advances, 2016, 6(7): 5761-5766.
- [12] LI X, LI Y Y, CHEN X Y, et al. Optically monitoring mineralization and demineralization on photoluminescent bioactive nanofibers[J]. Langmuir, 2016, 32(13): 3226-3233.
- [13] SPALDINN A, FIEBIG M. The renaissance of magnetoelectric multiferroics[J]. Science, 2005, 309(5733): 391-392.
- [14] JIANG Z, PAN J, WANG B, et al. Two dimensional Z-scheme AgCl/Ag/CaTiO₃ nano-heterojunctions for photocatalytic hydrogen production enhancement[J]. Applied surface science, 2018, 436: 519-526.
- [15] OLIVEIRAL H, RAMIREZM A, PONCEM A, et al. Optical and gas-sensing properties, and electronic structure of the mixed-phase CaCu₃Ti₄O₁₂/CaTiO₃ composites[J]. Materials research bulletin, 2017, 93: 47-55.
- [16] LI X, LI Y, CHEN X, et al. Optically monitoring mineralization and demineralization on photoluminescent bioactive nano-fibers[J]. Langmuir, 2016, 32(13): 3226-3233.
- [17] YAN Y X, YAN G H, ZHAO X X, et al. Enhanced photocatalytic activity of surface disorder-engineered CaTiO₃[J]. Materials research bulletin, 2018, 105: 286-290.
- [18] MAHATA M K, KOPPE T, MONDAL T, et al. Incorporation of Zn²⁺ ions into BaTiO₃: Er³⁺/Yb³⁺ nanophosphor: an effective way to enhance upconversion, defect luminescence and temperature sensing[J]. Physical chemistry chemical physics, 2015, 17(32): 20741-20753.
- [19] WANG Y L, ZHANG W T, ZHANG P C, et al. Effect of replacement of Ca by Zn on the structure and optical property of CaTiO₃: Eu³⁺ red phosphor prepared by sol-gel method[J]. Luminescence, 2015, 30(5): 533-537.
- [20] YANG X, WILLIAMS D, CHEN J, et al. Perovskite hollow cubes: morphological control, three-dimensional twinning and intensely enhanced photoluminescence[J]. Journal of materials chemistry, 2008, 18(30): 3543-3546.
- [21] YANG X, FU J, JIN C, et al. Formation mechanism of CaTiO₃ hollow crystals with different microstructures[J]. Journal of the American chemical society, 2010, 132(40): 14279-14287.